Biological Correlation of ^{18}F-FDG Uptake on PET in Pulmonary Neuroendocrine Tumors

KYOICHI KAIRA[1], HARUYASU MURAKAMI[1], MASAHIRO ENDO[2], YASUHISA OHDE[4], TATEAKI NAITO[1], HARUHIKO KONDO[4], TAKASHI NAKAJIMA[3], NOBUYUKI YAMAMOTO[1] and TOSHIAKI TAKAHASHI[1]

Divisions of [1]Thoracic Oncology, [2]Diagnostic Radiology, [3]Pathology, and [4]Thoracic Surgery, Shizuoka Cancer Center, Sunto-gun, Shizuoka, Japan

Abstract. *Background: It is widely recognized that pulmonary neuroendocrine tumors (PNET) include a spectrum that ranges from low-grade typical carcinoid (TC) and atypical carcinoid (AC) to high-grade large cell neuroendocrine carcinoma (LCNEC) and small cell lung carcinoma (SCLC). However, little is known about the usefulness of 2-[^{18}F]-fluoro-2-deoxy-D-glucose (^{18}F-FDG) positron-emission tomography (PET) in such tumors. We therefore, conducted a study including the analysis of the underlying biology of ^{18}F-FDG uptake. Materials and Methods: Thirty-four patients with early-stage PNETs who underwent ^{18}F-FDG PET before treatment were included in this study. Tumor sections were stained by immunohistochemistry for glucose transporter-1 (Glut1 and Glut3), hypoxia-inducible factor-1 alpha (HIF-1α), hexokinase-I, vascular endothelial growth factor (VEGF), microvessel density (MVD) determined by CD34 and (Akt)/mammalian target of rapamycin (mTOR) signaling pathway. Results: ^{18}F-FDG uptake correlated significantly with Glut1, HIF-1α, VEGF and CD34 expression. Uptake of ^{18}F-FDG tended to increase from low-grade to high-grade PNETs. Tumor metabolic activity was a useful marker for predicting postoperative prognosis in patients with early-stage PNETs. Conclusion: The amount of ^{18}F-FDG uptake is determined by the presence of glucose metabolism, hypoxia and angiogenesis.*

Neuroendocrine tumors (NETs) of the lung arise from Kulchitzky cells, which are normally present in the bronchial mucosa and share the common morphological features of neuroendocrine tumors, including organoid nesting, palisading, rosettes, or a trabecular growth pattern. These tumors are represented by a wide range of pathological entities (1-3). It is now widely recognized that such tumors of the lung include a spectrum including low-grade typical carcinoids (TC), intermediate-grade atypical carcinoids (AC), high-grade large cell neuroendocrine carcinomas (LCNEC) and small cell lung carcinomas (SCLC) (1-3). However, their clinicopathological profiles and relative grade of malignancy have not yet been defined (4-7). To ensure the appropriate choice of treatment for patients with various types of pulmonary neuroendocrine tumor (PNET), a histology-specific understanding of the clinicopathological behavior and prognosis is indispensable.

Recently, the usefulness of 2-[^{18}F]-fluoro-2-deoxy-D-glucose (^{18}F-FDG) positron emission tomography (PET) for the diagnosis of lung cancer has been investigated in many studies (8-10). Determination of malignant lesions with ^{18}F-FDG PET is based on their glucose metabolism (11, 12). The overexpression of glucose transporter-1 (GLUT1) has been shown to be closely related to ^{18}F-FDG uptake in human cancer (11, 12). GLUT1 is thought to be a possible intrinsic marker of hypoxia, and its expression has been found to be regulated by hypoxia *via* hypoxia inducible factor (HIF)-1-dependent means (13, 14). Previous studies suggest that hypoxic conditions correspond to higher ^{18}F-FDG uptake (15, 16). In addition, several researchers described the relationship between ^{18}F-FDG uptake and the expression of vascular endothelial growth factor (VEGF) or micro-vessel density (MVD) (17, 18). Hypoxia inducible factor (HIF) is considered to support tumor growth by the induction of angiogenesis *via* the expression of VEGF and also by anaerobic metabolic mechanisms (19). A preliminary report demonstrated that ^{18}F-FDG PET could be a valuable tool for assessing the effects of the mammalian target of rapamycin (mTOR) inhibition in patients with lung cancer (20). mTOR is a downstream component of the phosphoinositide-3-kinase (PI3K)/protein kinase B (AKT) pathway involved in the regulation of cell proliferation, angiogenesis, and metabolism. However, there is no report about the relationship between ^{18}F-FDG uptake within tumor cells and with the PI3K/AKT/mTOR signaling

Correspondence to: Kyoichi Kaira, MD, Division of Thoracic Oncology, Shizuoka Cancer Center, 1007 Shimonagakubo Nagaizumi-cho Sunto-gun, Shizuoka, 411-8777, Japan. Tel: +81 559895222, Fax: +81 559895634, e-mail: kkaira1970@yahoo.co.jp

Key Words: ^{18}F-FDG PET, pulmonary neuroendocrine tumor, GLUT1, hypoxia, angiogenesis, glucose metabolism.

pathway in human neoplasms. As many factors can influence the extent of ^{18}F-FDG uptake, the underlying mechanisms for ^{18}F-FDG accumulation are still a matter of debate in various human neoplasms. Although ^{18}F-FDG PET has been proven useful in detecting malignant pulmonary lesions, assessing treatment efficacy and in helping predict the prognosis of lung cancer, there is little evidence on the underlying biological mechanisms of ^{18}F-FDG uptake in PNETs. Defining a correlation between these biomarkers and ^{18}F-FDG uptake may lead to a better understanding and interpretation of ^{18}F-FDG PET scanning in pulmonary NE tumors. Therefore, we conducted the present study to investigate the biological correlation of ^{18}F-FDG on PET in pulmonary NE tumors.

Materials and Methods

Patients. Between March 2003 and October 2009, we analyzed 38 consecutive patients with PNETs who underwent ^{18}F-FDG PET and curative resection at the Shizuoka Cancer Center, Japan. Of these patients, four were excluded from further study because no tissue specimen was available. Thus, a total of 34 patients were analyzed in the study. All patients underwent lobectomy for clinical stage I disease. The clinical records of all patients were reviewed for prognosis after surgery. All PNETs had been diagnosed based on the definitions of the revised WHO classification of lung cancer (21). The Authors' approach to the evaluation and resection of these tumors has been described previously (7, 17). The study protocol was approved by the Institutional Review Board. There were 24 males and 10 females, and the median age was 70 years (range 51-78 years). Lobectomy had been performed in all patients. The postoperative pathological stage was determined according to the Union Internationale Contre le Cancer (UICC) staging system. The pathological diagnoses were: TC in five, AC in one, SCLC in 12 and LCNEC in 16. The median maximal tumor size was 26 mm (range: 11-60 mm). Twenty-three patients had pathological stage I disease and 11 patients had stage II disease. Adjuvant chemotherapy had been performed in 11 patients (seven treated with cisplatin plus etopiside and four with cisplatin plus irinotecan), and the remaining patients had undergone surgery alone. Patients underwent ^{18}F-FDG PET scanning before curative surgery. The median follow-up period was 24 months (range: 6-87 months); 19 patients were alive at the time of analysis, and 15 had died of disease recurrence. The median progression-free survival (PFS) was 14 months. The median follow-up period was as follows: for patients with TC and AC 65 months (range: 56-85 months); LCNEC 23 months (range: 9-75), and SCLC 21 months (range: 6-48 months).

^{18}F-FDG PET imaging. Patients fasted for at least four hours before ^{18}F-FDG PET examination. Patients received an intravenous injection of 200-250 MBq of ^{18}F-FDG and then rested for approximately one hour before undergoing imaging (22). Image acquisition was performed using an Advance NXi PET scanner and Discovery PET-CT scanner (GE Medical Systems, Milwaukee, WI, USA). Two-dimensional emission scanning was performed from the groin to the top of the skull. PET/CT images were independently reviewed by two experienced physicians. Acquired data were reconstructed by iterative ordered subset expectation maximization. To evaluate ^{18}F-FDG accumulation, the tumor was first examined visually, and then the peak standardized uptake value (SUV) of the entire tumor was determined. The region of interest (ROI), measuring 3 cm in diameter, was set at the mediastinum at the level of the aortic arch and the mean SUV of the mediastinum was calculated.

Immunohistochemical staining. Immunohistochemical staining was performed according to the procedure described in previous reports (22-25). The following antibodies were used: a rabbit polyclonal antibody against GLUT1 (AB15309, 1:200 dilution; Abcam, Tokyo, Japan); a rabbit polyclonal antibody against GLUT3 (AB15311, 1:100 dilution; Abcam); a rabbit monoclonal antibody against hexokinase I (AB55144, 1:200 dilution; Abcam); a mouse monoclonal antibody against HIF-1α (NB100-123, 1:50 dilution; Novus Biologicals, Inc., Littleton); a monoclonal antibody against VEGF (1:300 dilution; Immuno-Biological Laboratories Co.,Ltd., Japan); a mouse monoclonal antibody against CD34 (1:800 dilution; Nichirei, Tokyo, Japan); a mouse monoclonal antibody against epidermal growth factor receptor (EGFR) (1:100 dilution; Novovastra laboratories Ltd., Newcastle, UK); a rabbit polyclonal antibody against phosph-AKT (1:200 dilution; Abcam); a rabbit monoclonal antibody against phosph-mTOR (1:80 dilution; Cell Signaling); a rabbit monoclonal antibody against phosph-ribosomal-subunit-6 kinase (S6K) (1:100 dilution; Cell Signaling). The expression of GLUT1, GLUT3 and EGFR was considered positive if distinct membranous staining was present. Five fields (×400) were analyzed to determine the frequency of HIF-1α-stained nuclei and hexokinase I-stained cytoplasm. For GLUT1, GLUT3, EGFR, HIF-1α and hexokinase I, a semi-quantitative scoring method was used: 1= <10%, 2=10-25%, 3=25-50%, 4=51-75% and 5=>75% of positively stained cells. The tumors in which stained tumor cells made up more than 25% of the tumor were graded as positive. The expression of VEGF was quantitatively assessed according to the percentage of immunoreactive cells in a total of 1000 neoplastic cells. The number of CD34-positive vessels was counted in four selected hot spots in a ×400 field (0.26 mm^2 field area). Microvessel density (MVD) was defined as the mean count of microvessels per 0.26 mm^2 field area. p-AKT, p-mTOR and p-S6K were considered positive if membranous and/or cytoplasmic staining was present. For p-AKT, p-mTOR and p-S6K, a semi-quantitative scoring method was used: 1=<10%, 2=10-25%, 3=25-50%, 4=51-75% and 5=>75% of positively stained cells. The tumors in which stained tumor cells made up more than 25% of the tumor were graded as positive. Sections were assessed using a light microscope in a blinded fashion by at least two of the Authors.

Statistical analysis. Probability values of <0.05 indicated a statistically significant difference. Fisher's exact test was used to examine the association of two categorical variables. Correlation of different variables was analyzed using the nonparametric Spearman's rank test. The Kaplan-Meier method was used to estimate survival as a function of time, and survival differences were analyzed by the log-rank test. Statistical analysis was performed using JMP 8 for Windows (SAS, Institute Inc., Cary, NC, USA).

Results

^{18}F-FDG PET findings. The mean (±standard deviation) SUV_{max} of pulmonary carcinoid (TC and AC), LCNEC and SCLC was 2.8±1.9 (range: 1.6 to 6.5), 13.7±7.4 (range: 5.0

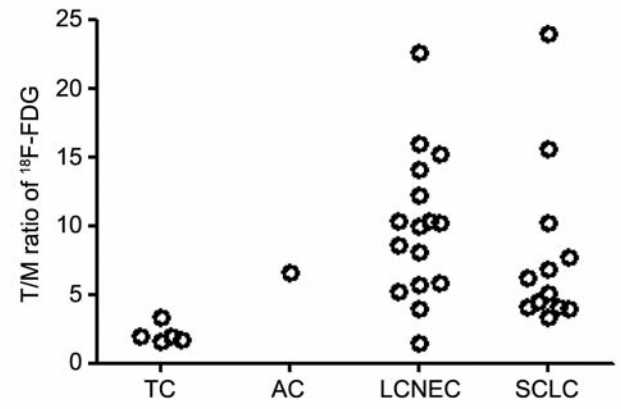

Figure 1. *Scatter plots of the Tumor/Mediastinum (T/M) ratio of the pulmonary neuroendocrine tumors analyzed in this study. TC, Typical carcinoid; AC, Typical carcinoid; LCNEC, large cell neuroendocrine carcinoma; and SCLC, small cell carcinoma.*

to 31.9) and 11.6±8.2 (range: 5.4 to 29.4), respectively. The SUV_{max} was significantly higher in LCNEC (p=0.005) and SCLC (p=0.048) than in pulmonary carcinoid, demonstrating no significant difference between LCNEC and SCLC (p=0.361). The scatter plots of the SUV_{max} of the PNETs are illustrated in Figure 1. The median value of SUV_{max} in PNETs was 9.3, and this value was used as the cut-off SUV_{max} in subsequent analyses. An SUV_{max} of more than 9.3 was defined as high uptake.

Immunohistochemical analysis. GLUT1 and GLUT3 were detected in tumor cells and localized predominantly on their plasma membrane. Positive rate of GLUT1 and GLUT3 expression was recognized in 79.4% (27/34) and 11.7% (4/34), respectively. Positive expression of HIF-1α was predominantly recognized in the cytoplasm with some nuclear staining, and was recognized in 85.2% (29/34). A positive expression of hexokinase-I was recognized in the cytoplasm and/or membrane of neoplastic cells, and was recognized in 58.8% (20/34). The median rate of VEGF positivity was 11.0% (range: 1-60%), and the median number of CD34-positive cells per field was 28 (range: 4-54). Positive expression of EGFR, p-AKT, p-mTOR and p-S6K was found in 70.5% (24/34), 26.4% (9/34), 29.4% (10/34) and 32.3% (11/34), respectively.

The positive rate of these biomarkers according to histological types is listed in Table I. The positive rate of GLUT1 expression was significantly higher in LCNEC (p=0.004) and SCLC (p=0.004) than TC and AC, demonstrating no significant difference between LCNEC and SCLC. The positive expression of HIF-1α was significantly higher in SCLC than TC and AC (p=0.024), demonstrating no significant difference between LCNEC and TC and AC.

Table I. *Positive rate of biomarkers according to histological type.*

Biomarker	Total (n=34)	TC+AC (n=6)	LCNEC (n=16)	SCLC (n=12)
GLUT1	79.4% (27/34)	16.6% (1/6)	87.5% (14/16)	91.6% (11/12)
GLUT3	11.7% (4/34)	16.6% (1/6)	18.7% (3/16)	0.0% (0/12)
Hexokinase I	58.8% (20/34)	50.0% (3/6)	75.0% (12/16)	41.6% (5/12)
HIF-1α	85.2% (29/34)	50.0% (3/6)	87.5% (14/16)	100% (12/12)
VEGF	44.1% (15/34)	16.6% (1/6)	62.5% (10/16)	33.3% (4/12)
CD34	41.1% (14/34)	16.6% (1/6)	50.0% (8/16)	41.6% (5/12)
EFGR	70.5% (24/34)	83.3% (5/6)	56.2% (9/16)	83.3% (10/12)
p-AKT	26.4% (9/34)	16.6% (1/6)	37.5% (6/16)	16.6% (2/12)
p-mTOR	29.4% (10/34)	33.3% (2/6)	50.0% (8/16)	0.0% (0/12)
p-S6K	32.3% (11/34)	16.6% (1/6)	50.0% (8/16)	16.6% (2/12)

TC, Typical carcinoid; LCNEC, large cell neuroendocrine carcinoma; SCLC, small cell carcinoma; GLUT1, glucose transporter-1; GLUT3, glucose transporter-3; VEGF, vascular endothelial growth factor; EGFR, epidermal growth factor receptor; mTOR, mammalian target of rapamycin; HIF-1α, hypoxia inducible factor-1α; p-AKT, phosphorylation of protein kinase B; S6K, ribosomal-subunit-6 kinase; CD34, microvessel density.

No statistically significant difference in the positivity of the other biomarkers was recognized among these histological types. Representative figures show ^{18}F-FDG PET findings and immunohistochemical results for PNETs are shown in Figures 2 and 3.

Relationship between ^{18}F-FDG uptake and different variables. The results of the statistical correlation between SUV_{max} and different variables are listed in Table II. High uptake of ^{18}F-FDG was significantly associated with high-grade malignancy, GLUT1, VEGF and CD34 positivity. Using Spearman rank correlation, the SUV_{max} was significantly correlated with GLUT1, HIF-1α, VEGF and CD34 (Table III).

Survival analysis. A statistically significant difference in the postoperative overall survival (OS) (p=0.042) was observed between patients with a low SUV_{max} and those with a high SUVmax on ^{18}F-FDG PET (Figure 4). Moreover, no statistically significant difference in OS (p=0.113) was recognized between patients with and these without adjuvant chemotherapy. In the analysis according to molecular

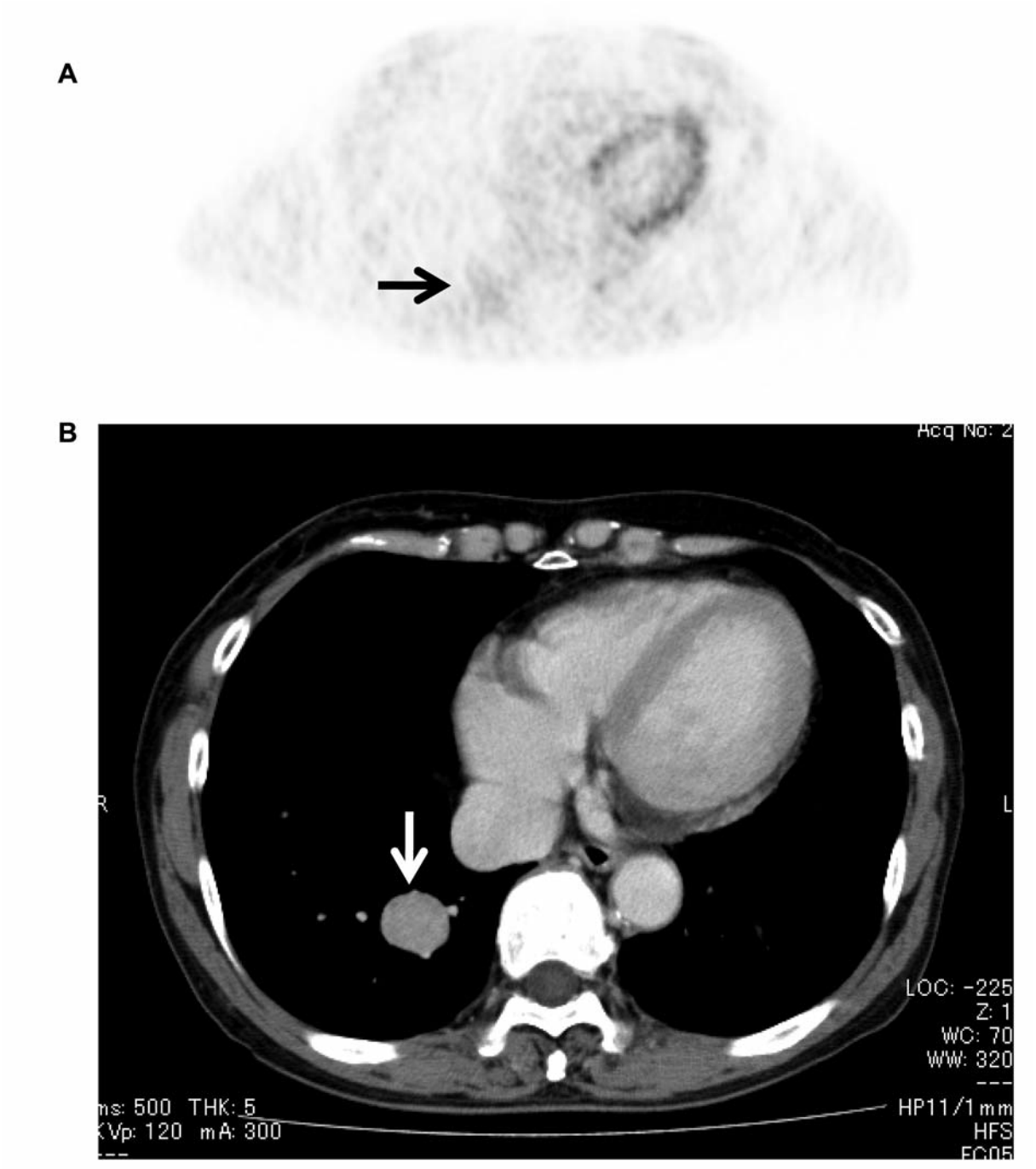

Figure 2. *Continued*

markers, the patients with positive GLUT1 expression had a significantly poorer OS (p=0.047) than those with negative GLUT1 expression (Figure 4). No statistically significant difference in survival was recognized for the other biomarkers.

Discussion

In this study, we evaluated the relationship between ^{18}F-FDG uptake and molecular biomarkers in patients with early-stage PNETs. The mechanism of ^{18}F-FDG uptake within tumor

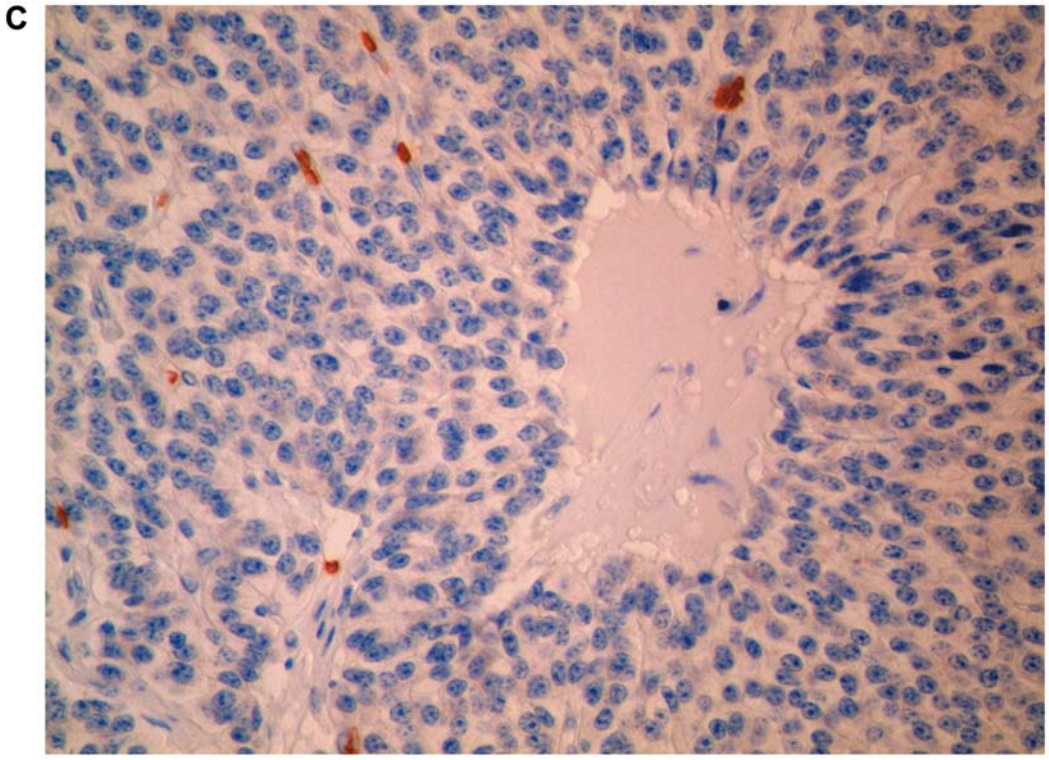

Figure 2. *Transaxial (A) sections of ^{18}F-FDG PET of a 67-year-old man with typical carcinoid of the right lung (p-T2N0M0). PET shows weak 2-[^{18}F]-fluoro-2-deoxy-D-glucose (^{18}F-FDG) accumulation in the lower right lobe (arrow), which is depicted on computed tomography (CT) scan (B) (arrow). The scoring of glucose transporter-1 (GLUT1) immunostaining was grade 2 and was membranous (C).*

Table II. *Relationship between Tumor/Mediastinum (T/M) ratio of 2-[^{18}F]-fluoro-2-deoxy-D-glucose (^{18}F-FDG) uptake and different variables.*

Variables		T/M ratio		
		High (n=17)	Low (n=17)	*p*-Value
Age	(≤65/>65 years)	6/11	3/14	0.438
Gender	(Male/female)	12/5	12/5	1.000
Pathological stage	(I/II)	11/6	12/5	1.000
Maximal size of tumor	(≤26/>26 mm)	6/11	12/5	0.084
Histological feature	(TC+AC/ SCLC+LCNEC)	0/17	6/11	0.018
Pleural involvement	(Positive/Negative)	7/10	3/14	0.258
Vascular invasion	(Positive/Negative)	13/4	7/10	0.079
Lymphatic permeation	(Positive/Negative)	9/8	6/11	0.498
GLUT 1	(Positive/Negative)	17/0	9/8	0.003
GLUT 3	(Positive/Negative)	2/15	2/15	1.000
Hexokinase-I	(Positive/Negative)	12/5	14/3	0.688
HIF-1α	(Positive/Negative)	16/1	14/3	0.601
VEGF	(Positive/Negative)	12/5	4/13	0.015
CD34	(Positive/Negative)	14/3	1/16	<0.001
EGFR	(Positive/Negative)	11/6	13/4	0.708
p-AKT	(Positive/Negative)	6/11	3/14	0.438
p-mTOR	(Positive/Negative)	7/10	3/15	0.146
p-S6K	(Positive/Negative)	6/11	5/12	1.000

Glut1, Glucose transporter-1; Glut3, glucose transporter-3; VEGF, vascular endothelial growth factor; EGFR, epidermal growth factor receptor; mTOR, mammalian target of rapamycin; TC, typical carcinoid; AC, atypical carcinoid; SCLC, small-cell lung cancer; LCNEC. Large cell neuroendocrine carcinoma; HIF-1α, hypoxia inducible factor-1α; p-AKT, phosphorylation of protein kinase B; S6K, ribosomal-subunit-6 kinase; CD34, microvessel density.

Table III. *Relationship between 2-[^{18}F]-fluoro-2-deoxy-D-glucose (^{18}F-FDG) uptake and biomarkers.*

Biomarkers	Spearman-γ	95% Confidence interval	*p*-Value
GLUT1	0.7741	0.5837-0.8838	<0.0001
GLUT3	0.3370	–0.0118-0.6127	0.0513
Hexokinase I	0.2457	–0.1112-0.5465	0.1614
HIF-1α	0.4470	0.1179-0.6877	0.0080
VEGF	0.4576	0.1310-0.6946	0.0065
CD34	0.7639	0.5670-0.8763	<0.0001
EFGR	0.0413	–0.3105-0.3833	0.8164
p-Akt	0.0891	–0.2666-0.4234	0.6163
p-mTOR	–0.0059	–0.3526-0.3422	0.9735
p-S6K	0.1614	–0.1971-0.4818	0.3618

GLUT1, Glucose transporter-1; GLUT3, glucose transporter-3; VEGF, vascular endothelial growth factor; EGFR, epidermal growth factor receptor; mTOR, mammalian target of rapamycin; HIF-1α; hypoxia inducible factor-1α; p-AKT, phosphorylation of protein kinase B; S6K, ribosomal-subunit-6 kinase; CD34, microvessel density.

cells was closely-associated with glucose metabolism (GLUT1), hypoxia (HIF-1α) and angiogenesis (VEGF and MVD). High uptake of ^{18}F-FDG was observed in patients with high-grade malignancy such as LCNEC or SCLC. In early-stage PNETs, ^{18}F-FDG uptake and GLUT1 expression were significantly correlated with poor outcome after curative surgery. In paticular, ^{18}F-FDG uptake within tumor cells was closely-correlated with the expression of GLUT1. Previous studies have documented that the amount of ^{18}F-FDG uptake in human neoplasms is determined by the presence of glucose metabolism (GLUT1), hypoxia (HIF-1α) and angiogenesis (VEGF and MVD) (12, 22-24). The results of our study correspond to those of previous studies.

Recently, Song *et al*. described that ^{18}F-FDG uptake was highly correlated with GLUT1 expression in PNETs (25). The results of their study suggest that GLUT1 expression plays a important role in determining ^{18}F-FDG uptake in these tumors. In their study, 32 patients underwent ^{18}F-FDG PET and the tumor sections were stained by immunohistochemistry for GLUT1 expression. For 12 patients (two SCLCs, five LCNECs and four carcinoids) surgically-resected tumors were analyzed, but for 20 patients with SCLC, expression was immunohistochemically examined in biopsy-tissue alone. Therefore, the amount of tumor specimen is one of their study limitations, and may bias the result of their study. Moreover, it is necessary to investigate markers of hypoxia to clarify the biological correlation of ^{18}F-FDG uptake.

Currently, paraffin-embedded specimens obtained by biopsy are the usual materials available for immunohistochemical analysis in SCLC. But these tumor samples are sometimes too small for the detection of molecular markers in heterogenous

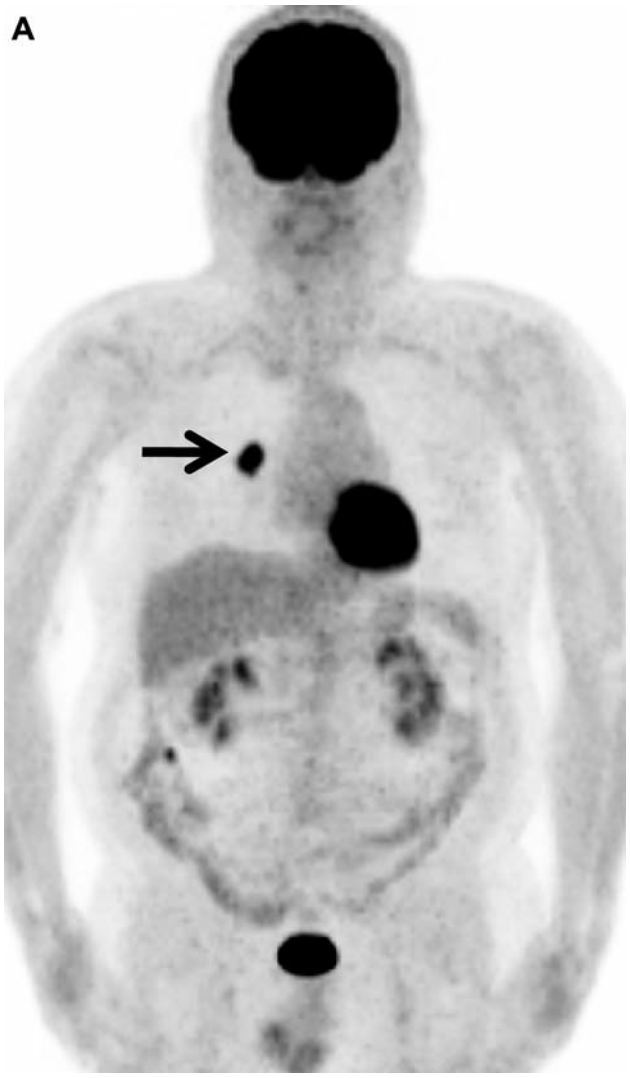

Figure 3. *Continued*

tumor tissue by immunohistochemistry, especially in SCLC or advanced LCNEC, and specimen biopsy may bias the immunohistochemical analysis of molecular biomarkers. Therefore, we used tumor samples obtained by the curatively intended resection of PNETs, and conducted the study to clarify whether ^{18}F-FDG uptake within NETs cell was correlated with markers of glucose metabolism and hypoxia. In our study, we found that markers of glucose metabolism and hypoxia were closely-correlated with ^{18}F-FDG uptake, but there was no direct correlation between ^{18}F-FDG uptake and expression of AKT/mTOR signaling pathway markers in these tumors.

GLUT1 and GLUT3 have been documented as being highly expressed in a variety of carcinomas (22, 26). However, there are only few reports on GLUT1 expression in PNETs. In the present study, GLUT1 expression was

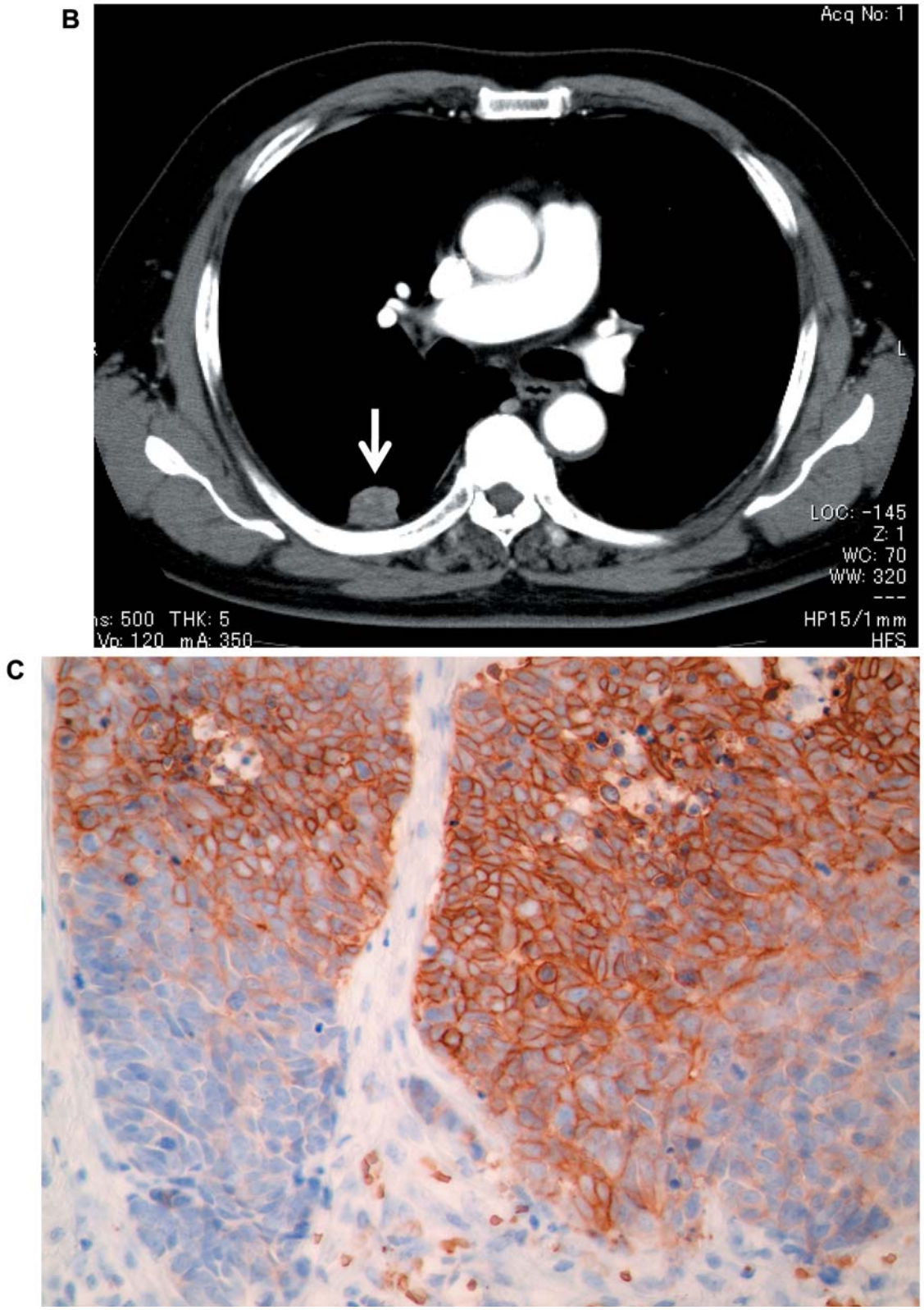

Figure 3. *Coronal (A) sections of ^{18}F-FDG PET of a 72-year-old man with small-cell lung cancer of the right lung (p-T2N0M0). PET shows increased 2-[^{18}F]-fluoro-2-deoxy-D-glucose (^{18}F-FDG) accumulation in the lower right lobe (arrow), which is depicted on CT scan (B) (arrow). Glucose transporter-1 (GLUT1) immunostaining showed a grade 4 scoring and was membrane-associated (C).*

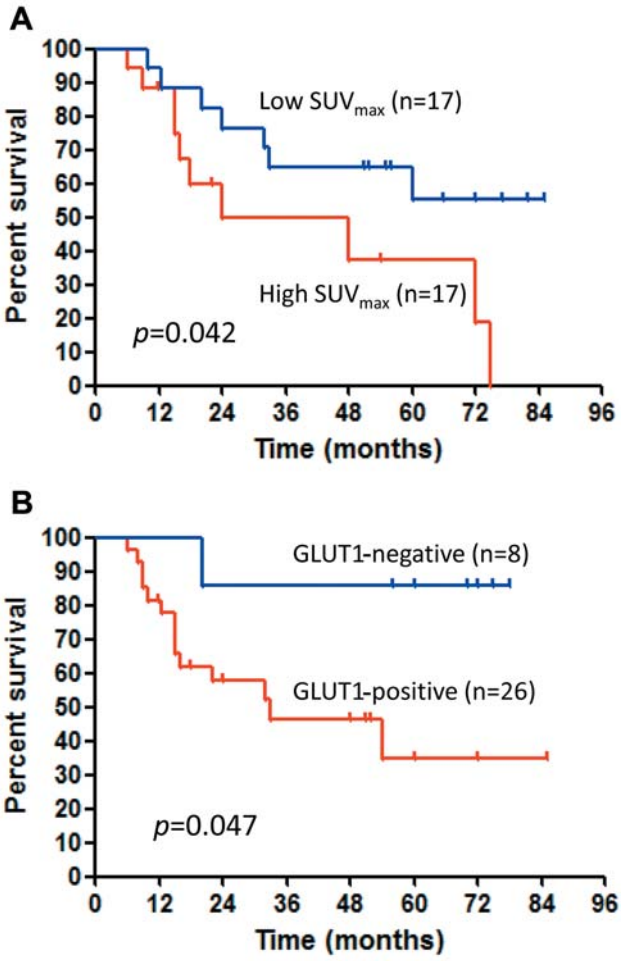

Figure 4. *Overall survival curve according to maximal standardized uptake value (SUV_{max}) of 2-[^{18}F]-fluoro-2-deoxy-D-glucose (^{18}F-FDG) uptake (A) and glucose transporter-1 (GLUT1) (B).*

useful for predicting the grade of malignancy and outcome, whereas GLUT3 expression was not associated with these factors: GLUT1 was highly expressed in patients with LCNEC and SCLC, but GLUT3 expression was low. Ozbudak *et al*. documented that GLUT1 expression was observed in 7% of TC, 74% of LCNEC and 78% of SCLC, and significantly correlated with neuroendocrine differentiation/tumor type and poor prognosis (27). In addition, a statistically significant difference in prognosis according to GLUT1 expression was seen for positive with stage I-II ($p<0.001$) but not stage III-IV ($p=0.40$) neuroendocrine carcinomas. Our study also indicated that Glut1 expression was closely-related to poor outcome in patients with stage I-II PNETs. Therefore, high uptake of ^{18}F-FDG and positive GLUT1 expression may have a prognostic significance in early-stage PNETs, but, further investigation is warranted.

According to tumor registry data, carcinoid tumors account for 1-2% of pulmonary neoplasms, LCNECs 3% and SCLCs 20% (1-4). Because these tumors comprise only a small proportion of total lines, there are only few reports on the ^{18}F-FDG PET findings of carcinoid and LCNEC. On the other hand, the majority of patients with SCLC are newly- diagnosed with advanced stage with local or distant metastases and are not appropriate for curative surgery. Thus, there are still no data on ^{18}F-FDG PET findings in patients with very early-stage SCLC. A previous report demonstrated that tumor metabolic activity assessed by ^{18}F-FDG PET is a significant prognostic factor in SCLC with limited and extensive disease (28). However, it remains unclear whether high tumor metabolic activity, as measured by ^{18}F-FDG PET, is associated with poor prognosis in very early-stage SCLC.

In vivo and *in vitro* studies demonstrated that there were high levels of GLUT1 protein and a correspondingly high ^{18}F-FDG uptake in two SCLC cell lines, and a similar co-upregulation of GLUT1 and VEGF was seen during hypoxia (29). This experimental data provides a further insight into our understanding of the crucial relationship between ^{18}F-FDG uptake, and glycolysis, hypoxia and angiogenesis. Moreover, Ioannou *et al*. found a significant correlation between HIF-1α and VEGF in 30 biopsy samples of SCLC and described that co-expression of HIF-1α and VEGF was associated with poor outcome (30). Our study also suggests that these markers of hypoxia play a crucial role in the uptake of ^{18}F-FDG in SCLC cells, and the expression of GLUT1 and HIF-1α significantly increases according to the grade of malignancy.

The present study has several limitations. Firstly, our population had a small sample size, and a heterogenous group of tumors. PNETs without SCLC are rare neoplasms, therefore the present findings warrant a larger, multi-center cohort study. Moreover, this small sample size may bias the evaluation of the relationship between ^{18}F-FDG uptake and postoperative outcome. Another limitation is that only cases with surgical treatment were collected to conduct an immunohistochemical study. In general, most patients with SCLC are not candidates for surgical resection because of local or systemic spread of the tumor. As the present study has investigated the patients with early-stage PNETs, the selected cases of SCLC here may not represent typical SCLC, which might have an aggressive nature.

In conclusion, the amount of ^{18}F-FDG uptake in early-stage PNETs is determined by markers of glucose metabolism, hypoxia and angiogenesis. Uptake of ^{18}F-FDG tended to increase from low-grade to high-grade PNETs. GLUT3, hexokinase I, EGFR, p-AKT, p-mTOR and p-S6K did not correlate significantly with ^{18}F-FDG uptake. However, glycolysis, hypoxia and angiogenesis may play an important role on the development of PNETs. The

relationship between ^{18}F-FDG uptake and these biomarkers may lead to a more rationale use of PET scan for patients with PNET.

Conflicts of Interest

We, all Authors, have no financial or personal relationships with other people or organizations that could inappropriately influence our work.

Acknowledgements

This work was supported in part by grant 21790793 (K. K) from the Ministry of Education, Culture, Sports, Science and Technology, Japan, and National Hospital Organization Policy Based Medical Services. We thank all staff of Pathology Department of Shizuoka Cancer Center for their technical assistance in immunohistochemical analysis.

References

1 Cooper WA, Thourani VH, Gal AA, Lee RB, Mansour KA and Miller JJ: The surgical spectrum of pulmonary neuroendocrine neoplasms. Chest *119*: 14-18, 2001.

2 Travis WD, Linnoila RI, Tsokos MG, Hitchcock CL, Cutler GB Jr, Nieman L, Chrousos G, Pass H and Doppman J: Neuroendocrine tumors of the lung with proposed criteria for large cell neuroendocrine carcinoma: an ultrastructural, immunohistochemical, and flow cytometric study of 35 cases. Am J Surg Pathol *15*: 529-553, 1991.

3 Travis WD, Rush W, Flieder DB, Falk R, Fleming MV, Gal AA and Gal AA and Koss MN: Survival analysis of 200 pulmonary neuroendocrine tumors with clarification of criteria for atypical carcinoid and its separation from typical carcinoid. Am J Surg Pathol *22*: 934-944, 1998.

4 Asamura H, Kameya T, Matsuno Y, Noguchi M, Tada H, Ishikawa Y, Yokose T, Jiang SX, Inoue T, Nakagawa K, Tajima K and Nagai K: Neuroendocrine neoplasms of the lung: a prognostic spectrum. J Clin Oncol *24*: 2470-2476, 2006.

5 Iyoda A, Hiroshima K, Toyozaki T, Haga Y, Fujisawa T, Ohwada H: Clinical characterization of pulmonary large cell neuroendocrine carcinoma and large cell carcinoma with neuroendocrine morphology. Cancer *91*: 1992-2000, 2001.

6 Takei H, Asamura H, Maeshima A, Suzuki K, Kondo H, Niki T, Yamada T, Tsuchiya R and Matsuno Y: Large cell neuroendocrine carcinoma of the lung: a clinicopathologic study of eighty-seven cases. J Thorac Cardiovasc Surg *214*: 285-292, 2002.

7 Kaira K, Ohde Y, Endo M, Nakagawa K, Okumura T, Takahashi T, Murakami H, Tsuya A, Nakamura Y, Naito T, Kondo H, Nakajima T and Yamamoto N: Expression of 4F2hc (CD98) in pulmonary neuroendocrine tumors. Oncol Rep *26*: 931-937, 2011.

8 Vansteenkiste JF, Stroobants SG, De Leyn PR, Dupont PJ, Bogaert J, Maes A, Deneffe GJ, Nackaerts KL, Verschakelen JA, Lerut TE, Mortelmans LA, Demedts MG: Lymph node staging in non-small-cell lung cancer with FDG-PET scan: a prospective study on 690 lymph node stations from 68 patients. J Clin Oncol *16*: 2142-2149, 1998.

9 Brock CS, Meikle SR and Price P: Dose fluorine-18 fluorodexyglucose metabolic imaging of tumor benefit oncology? Eur J Nucl Med *24*: 691-705, 1997.

10 Hoffman JM, Waskin HA, Schifter T, Hanson MW, Gray L, Rosenfeld S and Coleman RE: The use of FDG-PET in differentiating infectious from malignant central nervous system lesions in patients with AIDS. J Nucl Med *33*: 838, 1992.

11 Higashi K, Ueda Y, Sakurai A, Wang XM, Xu L, Murakami M, Seki H, Oguchi M, Taki S, Nambu Y, Tonami H, Katsuda S and Yamamoto I: Correlation of Glut-1 glucose transporter expression with [^{18}F] FDG uptake in non-small cell lung cancer. Eur J Nucl Med *27*: 1778-1785, 2000.

12 Chung JH, Cho KJ, Lee SS, Baek HJ, Park JH, Cheon GJ, Choi CW and Lim SM: Over expression of Glut 1 in lymphoid follicles correlates with false-positive ^{18}F-FDG PET results in lung cancer staging. J Nucl Med *45*: 999-1003, 2004.

13 Vleugel MM, Greijer AE, Shvarts A, van der Groep P, van Berkel M, Aarbodem Y, van Tinteren H, Harris AL, van Diest PJ and van der Wall E: Differential prognostic impact of hypoxia induced and diffuse HIF-1 alpha expression in invasive breast cancer. J Clin Pathol *58*: 172-177, 2005.

14 Elson DA, Ryan HE, Snow JW, Johnson R and Arbeit JM: Coordinate up-regulation of hypoxia inducible factor (HIF)-1a and HIF-1 target genes during multi-stage epidermal carcinogenesis and wound healing 1. Cancer Res *60*: 6189-6195, 2000.

15 Burgman P, Odonoghue JA, Humm JL and Ling CC: Hypoxia-induced increase in FDG uptake in MCF7 cells. J Nucl Med *42*: 170-175, 2001.

16 Thomas GV, Tran C, Mellinghoff IK, Welsbie DS, Chan E, Fueger B, Czernin J and : Sawyers CL: Hypoxia-inducible factor determines sensitivity to inhibitors of mTOR in kidney cancer. Nat Med *12*: 122-127, 2006.

17 Kaira K, Endo M, Shukuya T, Kenmotsu H, Naito T, Ono A, Tsuya A, Nakamua Y, Takahashi T, Murakami H, Kondo H, Nakajima T, Yamamoto N: ^{18}F-FDG uptake on PET could be a predictive marker of excision repair cross-complementation group 1 (ERCC1) expression in patients with thoracic neoplasms? Neoplasma *59*: 257-263, 2012.

18 Kaira K, Oriuchi N, Shimizu K, Ishikita T, Higuchi T, Imai H, Yanagitani N, Sunaga N, Hisada T, Ishizuka T, Kanai Y, Endou H, Nakajima T, Endo K and Mori M: Correlation of angiogenesis with ^{18}F-FMT and ^{18}F-FDG uptake in non-small cell lung cancer. Cancer Sci *100*: 753-758, 2009.

19 Ryan HE, Polni M, McNulty W, Elson D, Gassmann M, Arbeit JM and Johnson RS: Hypoxia-inducible factor-1α is a positive factor in solid tumor growth. Cancer Res *60*: 4010-4015, 2000.

20 Nogová L, Boellaard R, Kobe C, Hoetjes N, Zander T, Gross SH, Dimitrijevic S, Pellas T, Eschner W, Schmidt K, Bangard C, Hayes W, Thomas RK, Dietlein M, Giaccone G, Hoekstra OS, Lammertsma AA and Wolf J: Down-regulation of ^{18}FDG uptake in PET as an early pharmacodynamic effect in treatment of non-small cell lung cancer with the mTOR inhibitor everlimus. J Nucl Med *50*: 1815-1819, 2009.

21 Travis WD, Rush W and Flieder DB: International Histological Classification of Tumors, Histological Typing of Lung and Pleural Tumors, 1999.

22 Kaira K, Endo M, Abe M, Nakagawa K, Ohde Y, Okumura T, Takahashi T, Murakami H, Tsuya A, Nakamura Y, Naito T, Hayashi I, Serizawa M, Koh Y, Hanaoka H, Tominaga H, Oriuchi N, Kondo H, Nakajima T and Yamamoto N: Biologic correlation of 2-[^{18}F]-fluoro-2-deoxy-D-glucose uptake on positron emission tomography in thymic epithelial tumors. J Clin Oncol *28*: 3746-3753, 2010.

23 van Baardwijk A, Dooms C, van Suylen RJ, Verbeken E, Hochstenbag M, Dehing-Oberije C, Rupa D, Pastorekova S, Stroobants S, Buell U, Lambin P, Vansteenkiste J and De Ruysscher D: The maximum uptake of ^{18}F-deoxyglucose on positron emission tomography scan correlates with survival, hypoxia inducible factor-1α and GLUT-1 in non-small cell lung cancer. Eur J Cancer *43*: 1392-1398, 2007.

24 Riedl CC, Akhurst T, Larson S, Stanziale SF, Tuorto S, Bhargava A, Hricak H, Klimstra D and Fong Y: ^{18}F-FDG PET scanning correlates with tissue markers of poor prognosis and predicts mortality for patients after liver resection for colorectal metastases. J Nucl Med *48*: 771-775, 2007.

25 Song YS, Lee WW, Chung JH, Park SY, Kim YK and Kim SE: Correlation between FDG uptake and glucose transporter type 1 expression in neuroendocrine tumors of the lung. Lung Cancer *61*: 54-60, 2008.

26 Younes M, Brown RW, Stephenson M, Gondo M and Cagle PT: Over expression of Glut1 and Glut3 in stage I nonsmall cell lung carcinoma is associated with poor survival. Cancer *80*: 1046-1051, 1997.

27 Ozbudak IH, Shilo K, Tavora F, Rassaei N, Chu WS, Fukuoka J, Jen J, Travis WD and Franks TJ: Glucose transporter-1 in pulmonary neuroendocrine carcinomas: expression and survival analysis. Modern Pathol *22*: 633-638, 2009.

28 Lee YJ, Cho A, Cho BC, Yun M, Kim SK, Chang J, Moon JW, Park IK, Choi HJ and Kim JH: High tumor metabolic activity as measured by fluorodeoxyglucose positron emission tomography is associated with poor prognosis in limited and extensive stage small-cell lung cancer. Clin Cancer Res *15*: 2426-2432, 2009.

29 Pedersen MW, Holm S, Lund EL, Højgaard L and Kristjansen PE: Coregulation of glucose uptake and vascular endothelial growth factor (VEGF) in two small-cell lung cancer (SCLC) sublines *in vivo* and *in vitro*. Neoplasia *3*: 80-87, 2001.

30 Inoannou M, Papamichali R, Kouvaras E, Mylonis I, Vageli D, Kerenidou T, Barbanis S, Daponte A, Simos G, Gourgoulianis K and Koukoulis GK: Hypoxia inducible factor-1 alpha and vascular endothelial growth factor in biopsies of small cell lung carcinoma. Lung *187*: 321-329, 2009.

Received July 19, 2013
Revised September 12, 2013
Accepted September 13, 2013